Symposium on the Acoustics of Poro-Elastic Materials

Reflection and transmission by a double porosity layer obeying Berryman-Wang theory

F. KACHKOUCH, H. FRANKLIN, A. TINEL, A. ALEM, H. WANG

Université Le Havre Normandie, Laboratoire Ondes et Milieux Complexes LOMC

UMR CNRS 6294 - LabEx EMC³

PLAN

- Main objectives
- Double porosity model
- Transmission characteristics for a layer of Berea Sandstone
- Dispersion curves for Berea sandstone
- Evaluation of the clogging by ultrasonics testing
- Conclusion & prospects

Main objectives

- Characterization of double porosity layers by acoustic methods
- Accessibility to double porosity parameters (porosities, permeabilities, bulk modulus…)
- Evaluation of the clogging/pollution phenomenon due to the deposition of fine suspended particles resulting from a water flow caused by rainwater infiltration.
- Estimation of erosion.

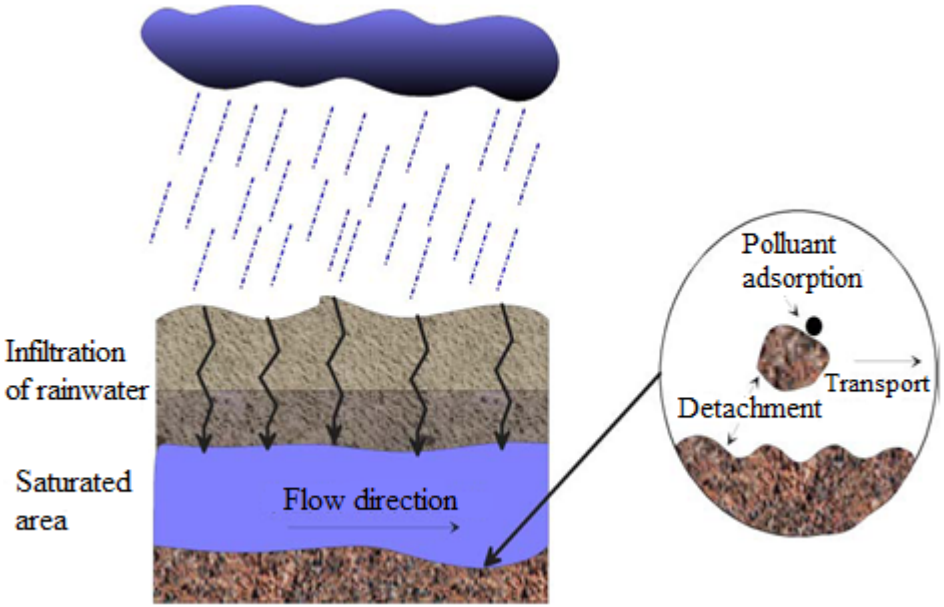

Double porosity model

- **Berea Sandstone (confirmed)**
- **Robu ©**

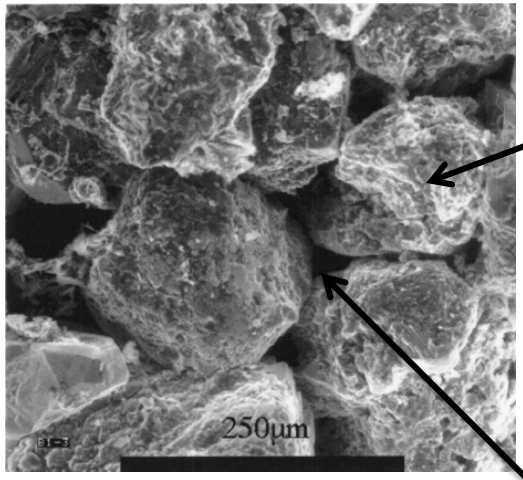

https://www.researchgate.net/figure/234848514_fig6_FIG-6-A-semilogarithmical-plot-of-the-FID-for-the-fully-water-saturated-Berea-sandstone

$\nu^{(1)}\ \phi^{(1)}$

Microporosity
(Matrix porosity)

$k_{22} > k_{11}$

$\nu^{(1)}\phi^{(1)} > \nu^{(2)}\phi^{(2)}$

$\nu^{(2)}\ \phi^{(2)}$

Macroporosity
(fractures porosity)

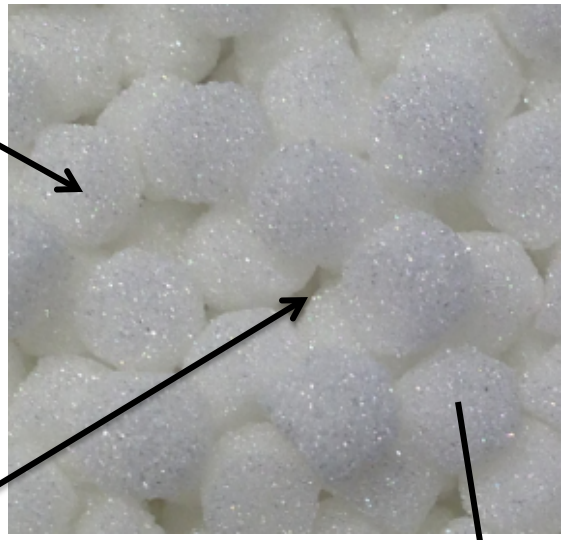

Porous Glass Beads Borosilicateglas
3.3 ROBU
(ϕ = 4mm)

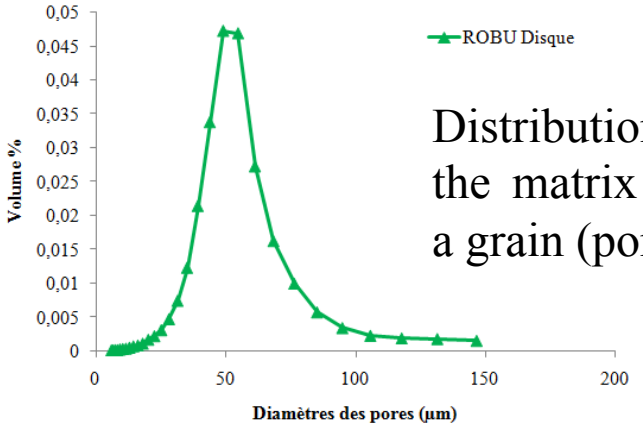

Distribution profile of the matrix porosity in a grain (porosimeter)

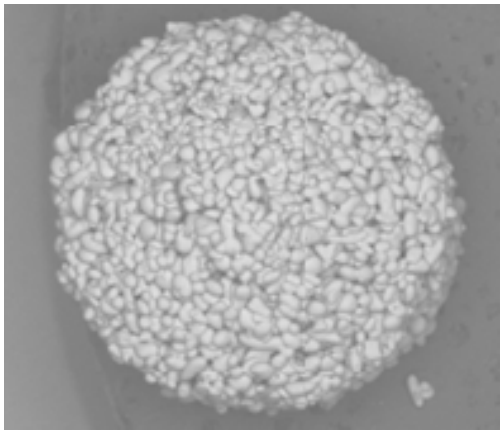

Views on Electronic scanning microscope

- **Hypothesis of double porosity medium (Berryman and Wang (Int. J. Rock Min. (2000))**

- Extension of Biot's theory to account for both pores and fractures (phenomenological)

- Continuous medium (low frequency waves considered)

- Isotropy (randomly oriented fractures, no preferred axis for fluid flow)

- Fluid in matrix and fractures is the same but the two fluid regions may be in different states of average stress (distinguished by their superscripts)

Consequence of this model : the increased number of independent coefficients describing the medium (inertial, drag and stress-strain) with respect to Biot's initial theory.

Alternative theory : C. Boutin and P. Royer Geophys. J. Int. (2015)

Match with Berryman and Wang theory at low frequency but more complicated to implement

➢ Constitutive equations for isotropic double porosity poroelastic medium

- Stress tensor and fluid pressures

$$\sigma_{\alpha\beta} = \left(H - 2\mu\right)\varepsilon_{\delta\delta}\delta_{\alpha\beta} + 2\mu\varepsilon_{\alpha\beta} - \left[C^{(1)}\xi^{(1)} + C^{(2)}\xi^{(2)}\right]\delta_{\alpha\beta}$$

$$P^{(1)} = -C_{12}e + C_{22}\xi^{(1)} + C_{23}\xi^{(2)}$$

$$P^{(2)} = -C_{13}e + C_{23}\xi^{(1)} + C_{33}\xi^{(2)}$$

H, $C^{(1)}$, $C^{(2)}$: moduli of the dPP medium depending on C_{ij}

C_{ij} : related to the material properties and to the generalized poroelastic expansion and storage coefficients

- Relative fluid-solid displacements

$$\boldsymbol{w}^{(1)} = \nu^{(1)}\phi^{(1)}\left(\boldsymbol{U}^{(1)} - \boldsymbol{u}\right)$$

$$\boldsymbol{w}^{(2)} = \nu^{(2)}\phi^{(2)}\left(\boldsymbol{U}^{(2)} - \boldsymbol{u}\right)$$

$\boldsymbol{u}$, $\boldsymbol{U}^{(1)}$, $\boldsymbol{U}^{(2)}$: the displacement vectors of the solid frame, the micropore fluid and the macropore fluid.

➢ Material data table

Parameters	Symbols and units	Berea sandstone (from BW Int. J. Rock Min. 2000)	Water
Density of grains	ρ_s (kg/m^3)	2600	
Unjacketed bulk modulus for the whole	K_s (GPa)	39	
Unjacketed bulk modulus for the matrix	$K_s^{(1)}$ (GPa)	38.306	
Total porosity	ϕ	0.1926	
Matrix porosity	$\phi^{(1)}$	0.178	
Fracture porosity	$\phi^{(2)}$	1	
Matrix permeability	$k^{(11)}$ (m^2)	10^{-16}	
Fracture permeability	$k^{(22)}$ (m^2)	10^{-12}	
Volume fraction occupied by matrix	$v^{(1)}$	0.9822	
Volume fraction occupied by fractures	$v^{(2)}$	0.0178	
Biot-Willis parameter for the whole	α	0.8462	
Biot-Willis parameter for the matrix	$\alpha^{(1)}$	0.7389	
Biot-Willis parameter for the fractures	$\alpha^{(2)}$	1	
Overall tortuosity	a	2.9460	
Matrix tortuosity	$a^{(1)}$	3.3090	
Fracture tortuosity	$a^{(2)}$	1	
Bulk modulus of undrained porous frame	K_u (GPa)	15.2	
Jacketed bulk modulus of matrix	K_1 (GPa)	10	
Jacketed bulk modulus of fractures	K_2 (GPa)	0.108	
Jacketed bulk modulus of porous frame	K (GPa)	6	
Shear modulus for drained medium	μ (GPa)	5.478	
Density	ρ_f (kg/m^3)		1000
Pore fluid bulk modulus	K_f (GPa)		2.3
Viscosity	η (Pa s)		10^{-3}

➢ Analytical model for Berea sandstone

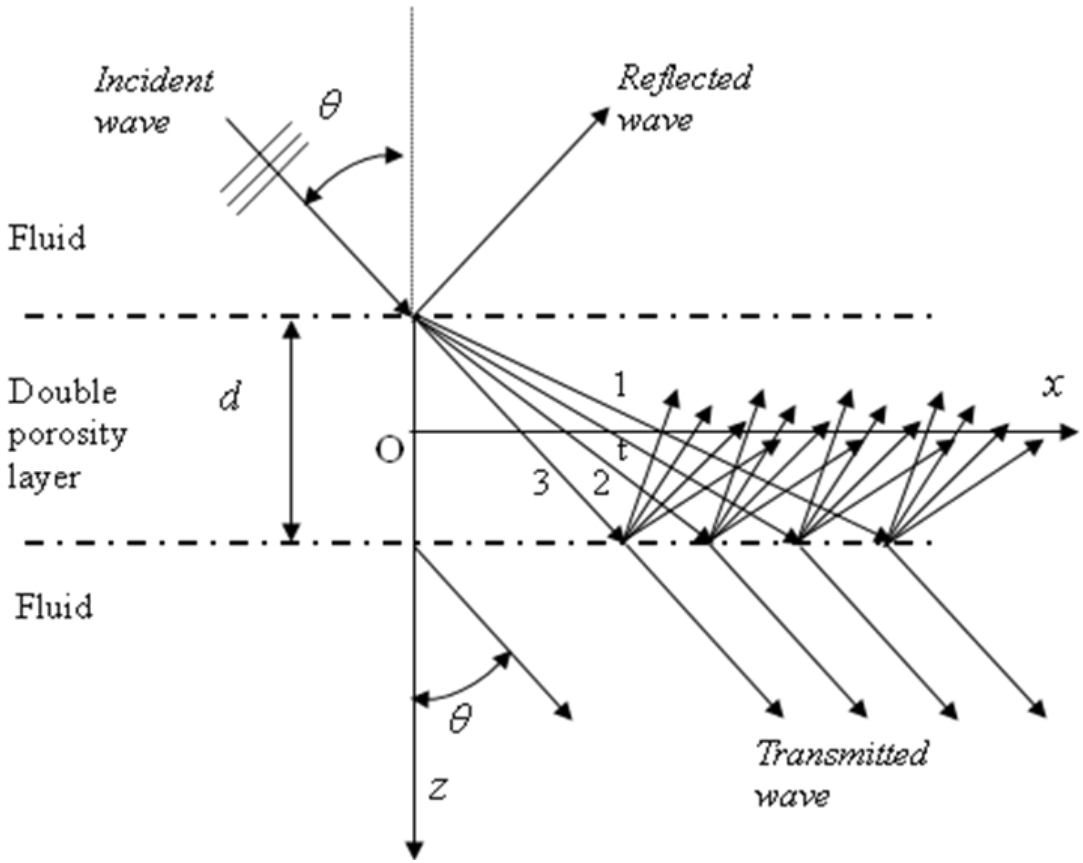

1, 2, 3: dilatational waves

t: shear wave

➢ Basic equations of Berryman-Wang theory

- **Boundary conditions (filtration occurs across the interfaces at z = ± d/2)**

$u_{0z} = u_z + w_z^{(1)} + w_z^{(2)}$	Continuity of fluid volume
$P_0 = P^{(1)}$	Continuity of fluid pressure for phase 1
$P_0 = P^{(2)}$	Continuity of fluid pressure for phase 2
$-P_0 = \sigma_{zz}$	Continuity of normal stress
$0 = \sigma_{xz}$	Disappearance of tangential stress

- **Reflection and transmission coefficients**

$$\begin{pmatrix} R \\ T \end{pmatrix} = \frac{1}{2}\begin{pmatrix} \dfrac{\sum_{cyc}\left(C_{S1} + i\tau_1\right)\mathrm{X}^{+}_{S23}}{\sum_{cyc}\left(C_{S1} - i\tau_1\right)\mathrm{X}^{-}_{S23}} & + & \dfrac{\sum_{cyc}\left(C_{A1} - i\tau_1\right)\mathrm{X}^{-}_{A23}}{\sum_{cyc}\left(C_{A1} + i\tau_1\right)\mathrm{X}^{+}_{A23}} \\ & - & \end{pmatrix}$$

$$\sum_{cyc}\left(C_{S1} + i\tau_1\right)\mathrm{X}^{+}_{S23} = \left(C_{S1} + i\tau_1\right)\mathrm{X}^{+}_{S23} + \left(C_{S2} + i\tau_2\right)\mathrm{X}^{+}_{S31} + \left(C_{S3} + i\tau_3\right)\mathrm{X}^{+}_{S12}$$

$$\mathrm{X}^{\pm}_{\bullet mn} = \begin{vmatrix} C^{(1)}_{\bullet Fm} \pm i\tau_m & C^{(1)}_{\bullet Fn} \pm i\tau_n \\ C^{(2)}_{\bullet Fm} \pm i\tau_m & C^{(2)}_{\bullet Fn} \pm i\tau_n \end{vmatrix}$$

• = S or A

(1), (2) : fluid phases

$$\begin{pmatrix} C_{SFm}^{(j)} \\ C_{AFm}^{(j)} \end{pmatrix} = \frac{\rho_{fm}^{(j)}}{\rho_t} l_t^2 L \begin{pmatrix} \cot\left(K_{mz}\, d/2\right) \\ \tan\left(K_{mz}\, d/2\right) \end{pmatrix}$$

They account for the squirting out and the suction of the saturating fluid under the effect of the compressional and shear deformations of the elastic frame.

$$\begin{pmatrix} C_{Sm} \\ C_{Am} \end{pmatrix} = LN_m \begin{pmatrix} \cot\left(K_{mz}\, d/2\right) \\ \tan\left(K_{mz}\, d/2\right) \end{pmatrix} + M_m \begin{pmatrix} \cot\left(K_{tz}\, d/2\right) \\ \tan\left(K_{tz}\, d/2\right) \end{pmatrix}$$

They account for the deformations of the elastic frame and express the coupling of each of the dilatational wave with the shear wave.

$$\boldsymbol{\tau}_m = \boldsymbol{\tau}_{m0} + \boldsymbol{\tau}_m^{(1)} + \boldsymbol{\tau}_m^{(2)}$$

It depends on several parameters constituting the medium as the density, and also on the acoustical properties as the wave numbers (perturbation of the Cs and Ca)

j=1, 2 (fluid phases), m=1, 2, 3 (wave numbers)

Transmission characteristics for a layer of Berea Sandstone

Complex « usual » modes obtained with real angles

K. E. Graff
Wave Motion in Elastic Solids 1975

Complex « unusual » modes obtained with imaginary angles

Measurable experimentally ??

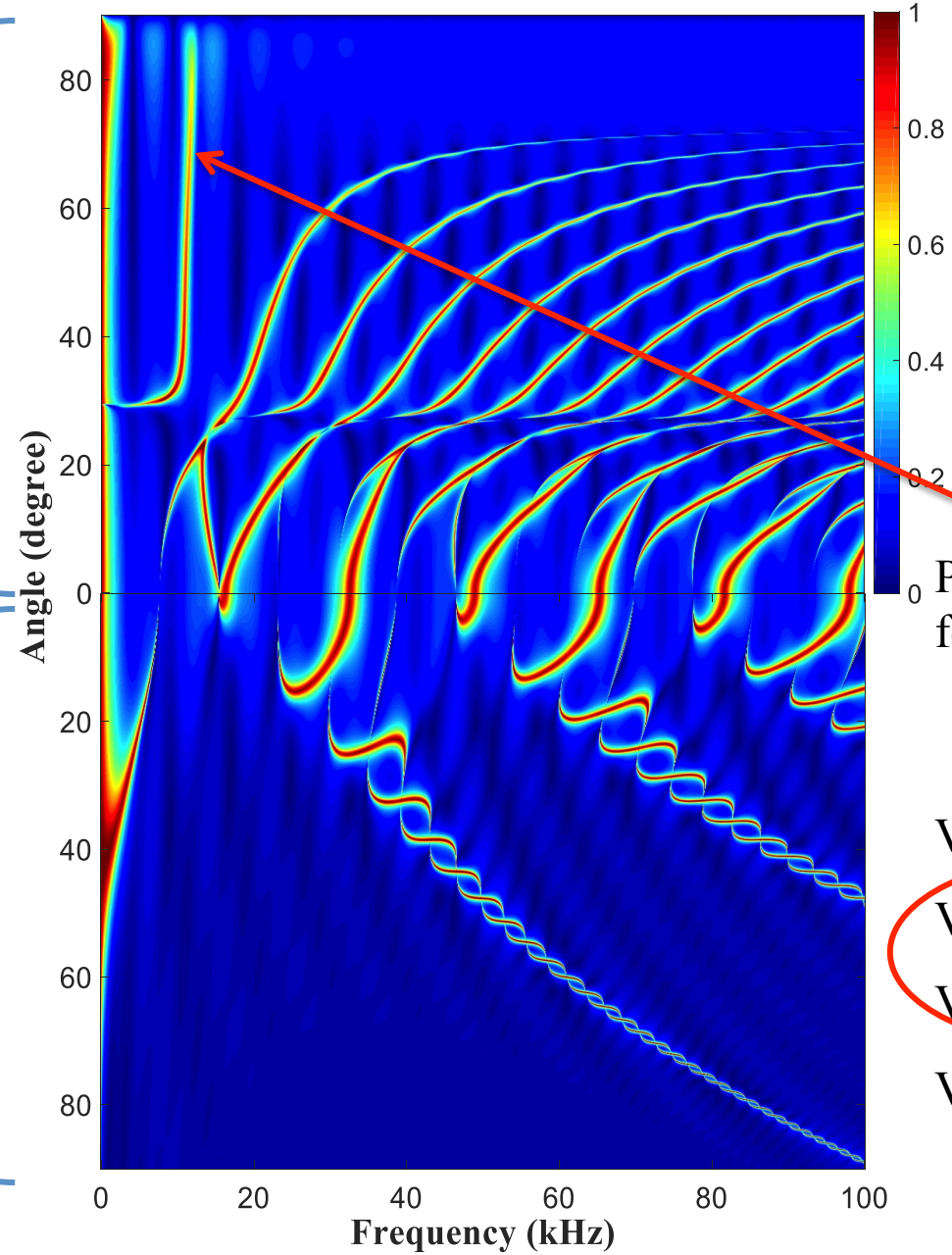

Absence of A0-like mode ???

Partial branch only for S0

V_{1max} = 3270 m/s

V_{2max} = 550 m/s

V_{3max} = 35 m/s

V_{tmax} = 1552 m/s

Dispersion curves for Berea sandstone

- **Obtained with the transition operator**

in relation with symmetrical modes

$$T_S = (R + T - 1)/2i$$

Enhancement of the vertical mode visualisation (related to the second dilatational wave)

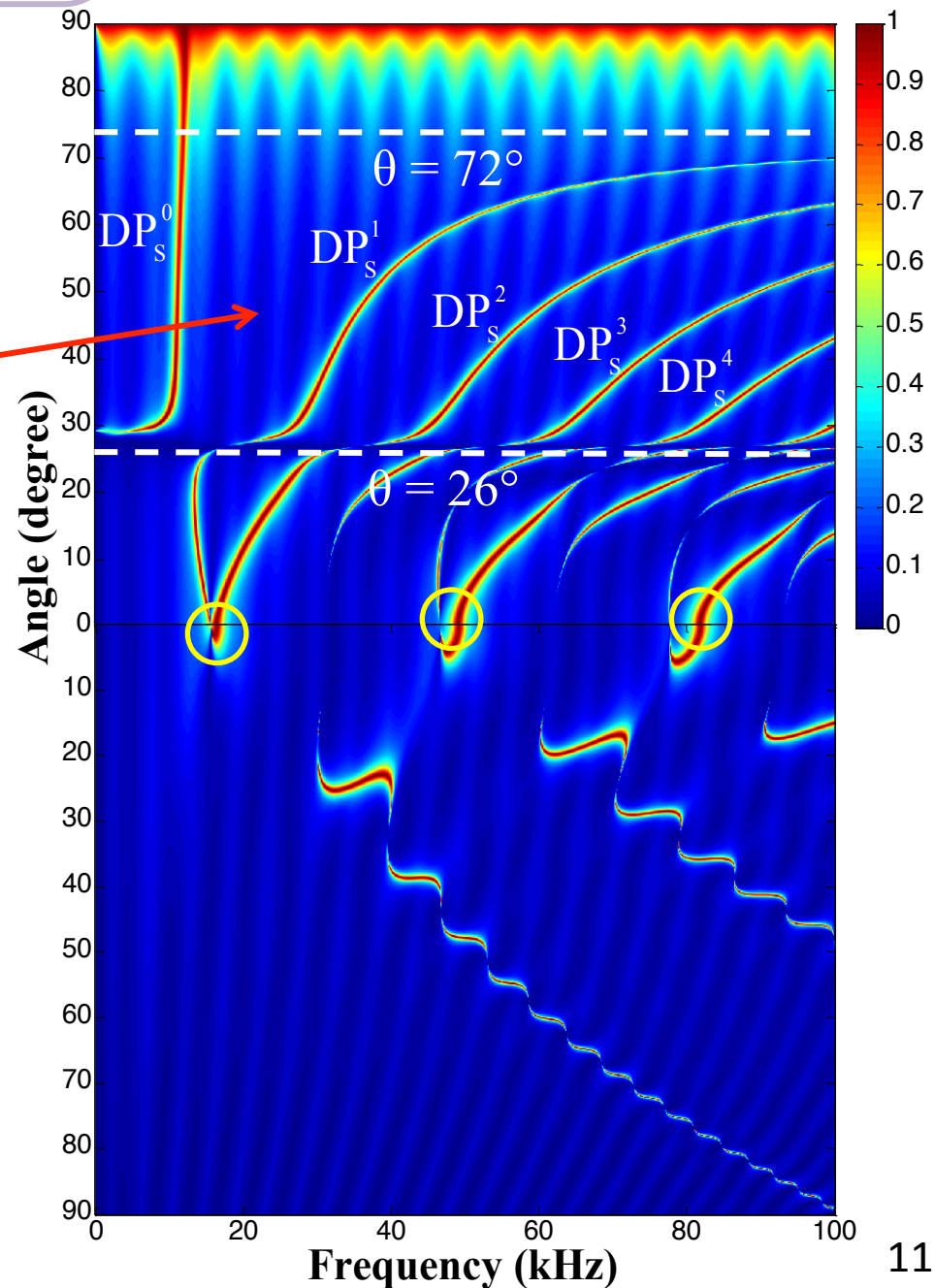

Cut-off frequencies for symmetrical modes

$$f_{jk} = \left(k + \tfrac{1}{2}\right) c_j / d \qquad f_{tk} = k\, c_t / d$$

k = positive integer
j = 1, 2, 3

$$f_{10} = 16351, \quad f_{11} = 49053, \quad f_{12} = 81756, \ldots$$

$$f_{t0} = 15520, \quad f_{t1} = 31040, \quad f_{t2} = 46560, \quad f_{t3} = 62080, \ldots$$

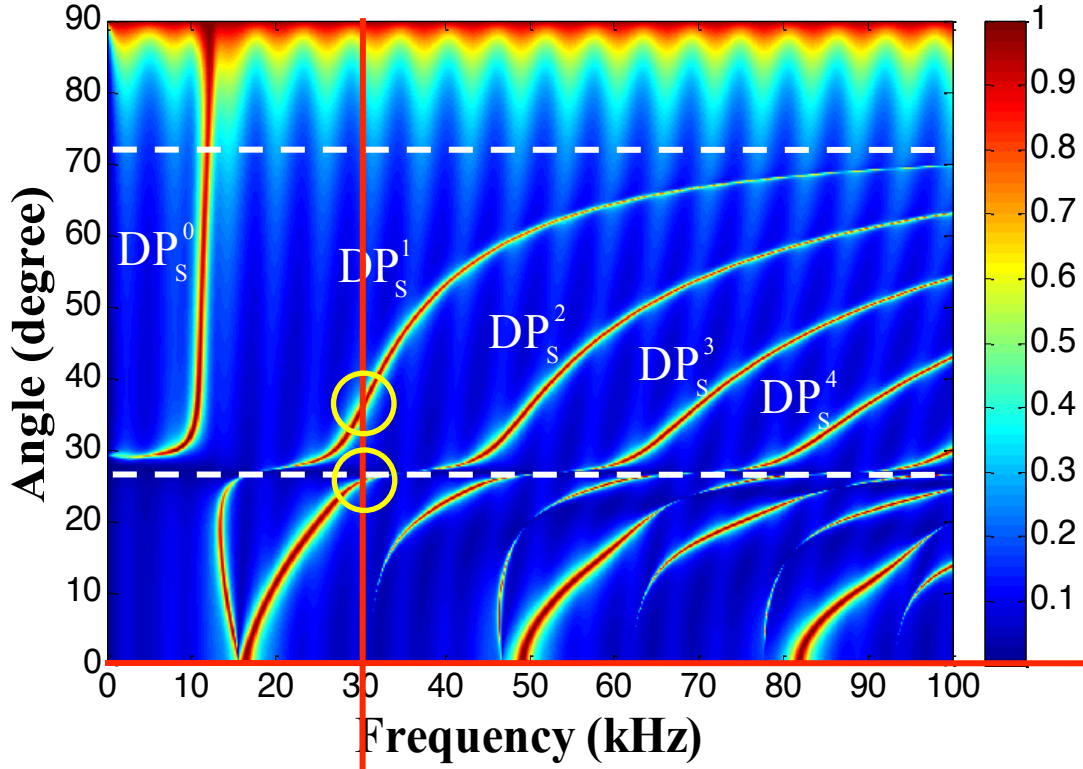

First dilatational wave

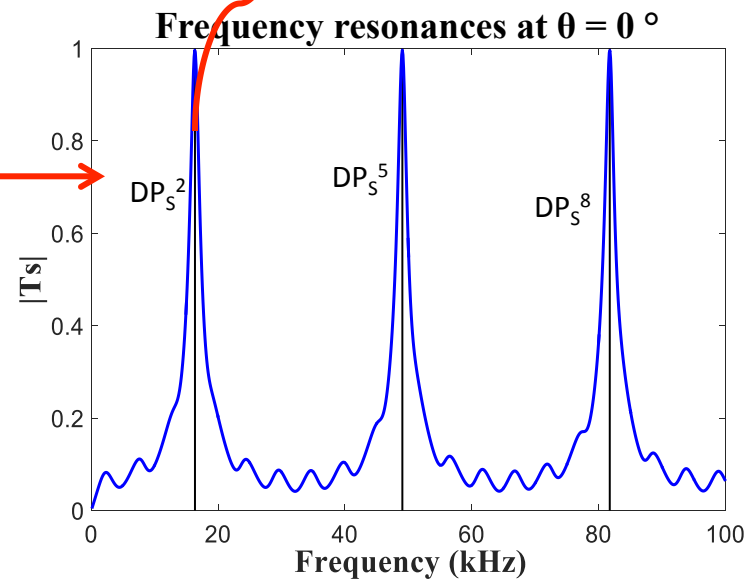

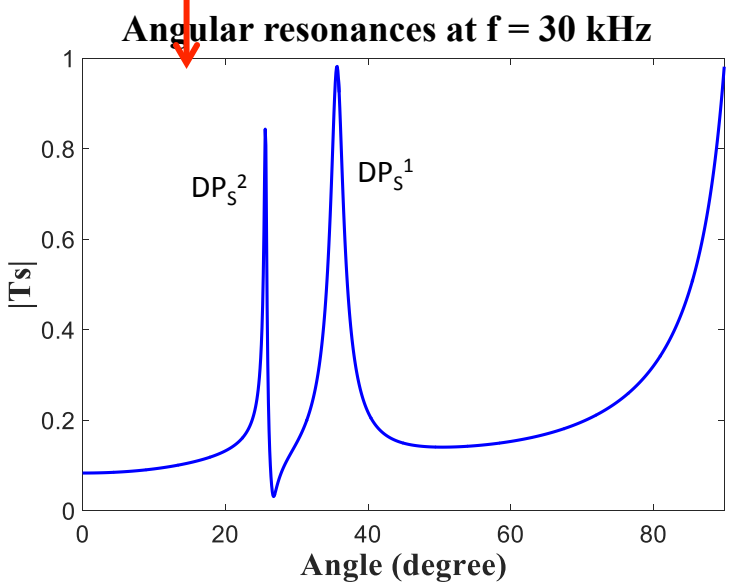

Absence of spikes corresponding to the shear wave because of their small width of resonance

➢ Effect of the total porosity variation on the transmission coefficient

$\phi_t = 19\%$

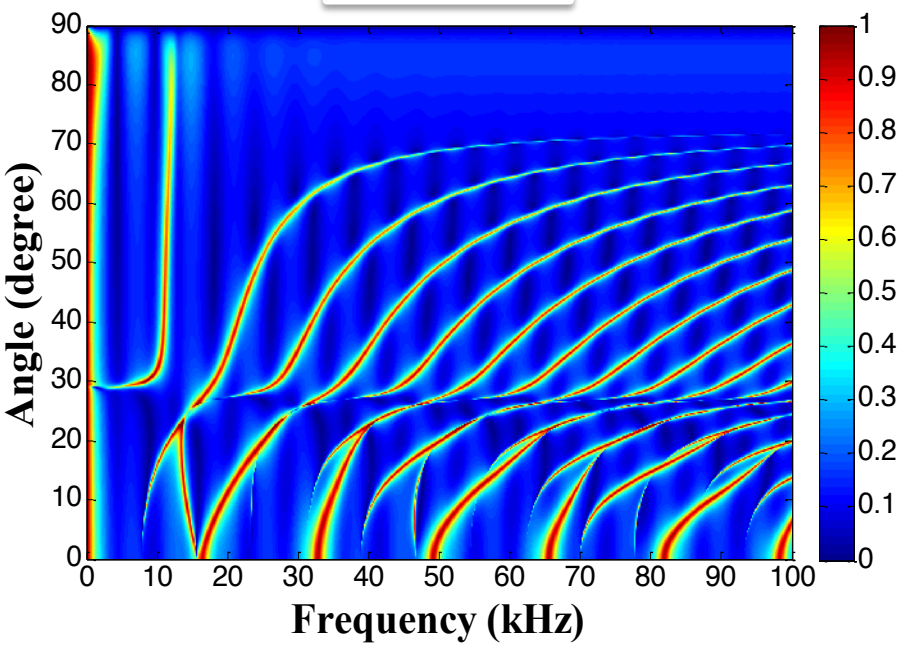

$\phi_t = 10\%$

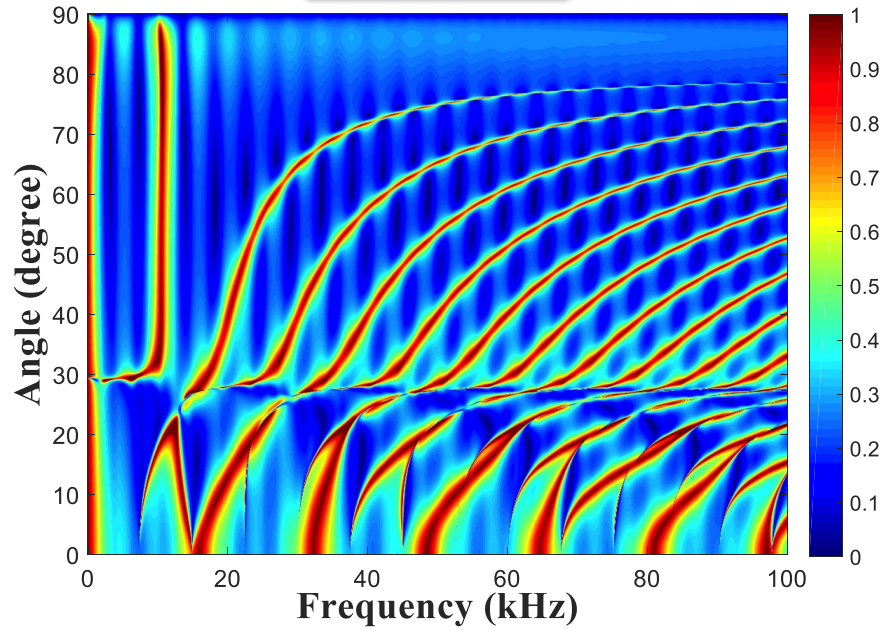

- The spikes shift toward the low frequecy
- The resonance width is more larger for a small porosity

➢ Effect of permeabilities variation on the transmission coefficient

$k_{22} = 10^{-12}$ m², $k_{11} = 10^{-16}$ m²

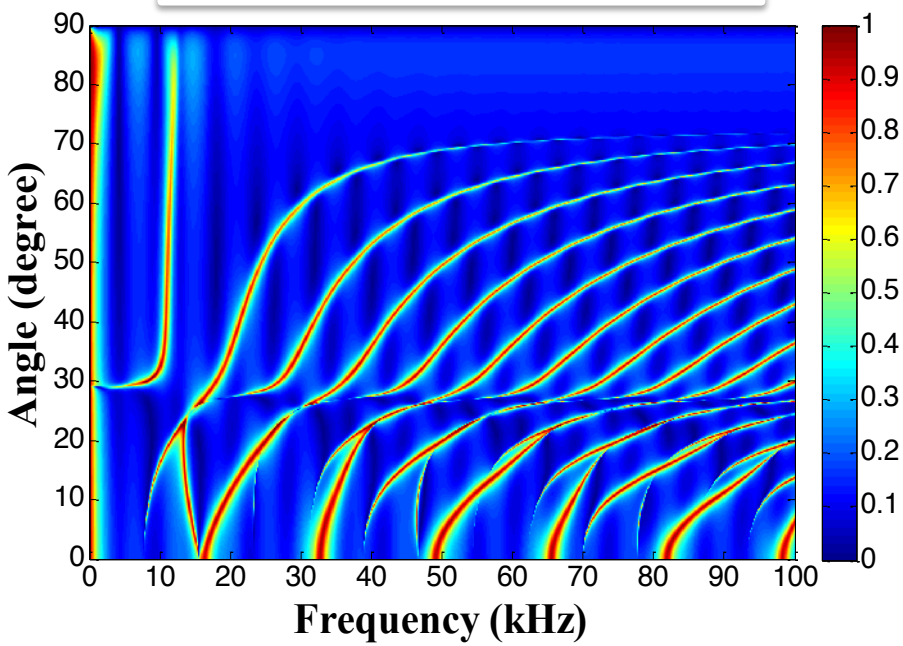

$k_{22} = 10^{-10}$ m², $k_{11} = 10^{-14}$ m²

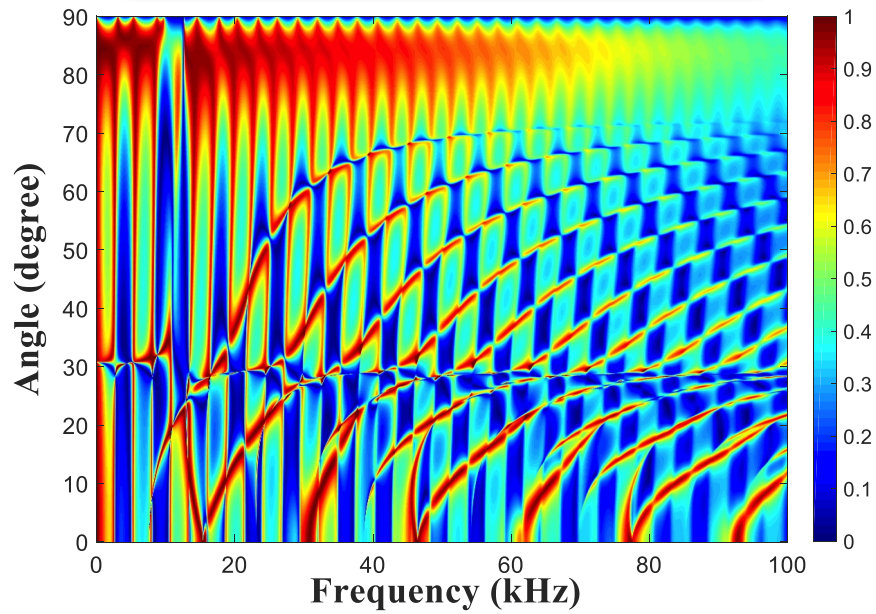

- The spikes shift toward the low frequecy
- The increase of the transmission amplitude (above the second critical angle)

For prospects : study of parameters affecting the propagation of Lamb modes

Evaluation of the clogging by ultrasonics testing

- **Model for handling a layer of granular medium (Robu)**

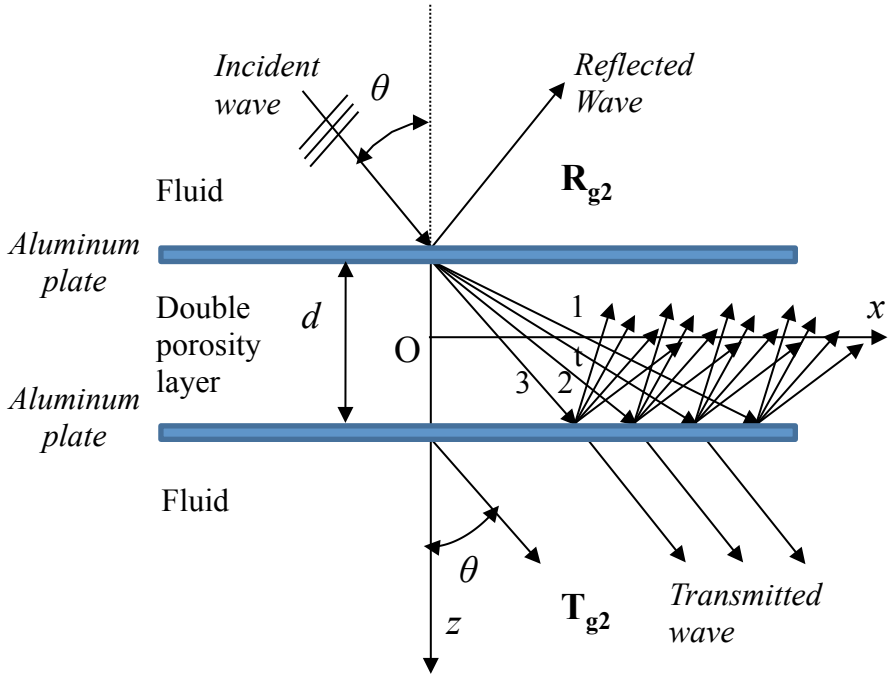

Fluid – Aluminium plate – fluid

Fluid – DPP – fluid (previous study)

R_{g1}, T_{g1}

Fluid – Aluminium plate – fluid → R_p, T_p

D = 0 ⇒ The model presented

- **Fabry-Perot method :**

$$R_{g2} = R_{g1} + \frac{(T_{g1})^2 R_p}{1 - R_{g1} R_p}$$

$$T_{g2} = \frac{T_{g1} T_p}{1 - R_{g1} R_{dpp}}$$

Characterization of the clogging by injecting fines particles of clay with a water flow

coefficients

$$C_{\exp} = \frac{S}{S_0}$$

FFT of the temporel signal transmitted through the model filled with DPP

FFT of the temporel signal transmitted through the model filled with water

$$C_{num} = \frac{T}{T_0}$$

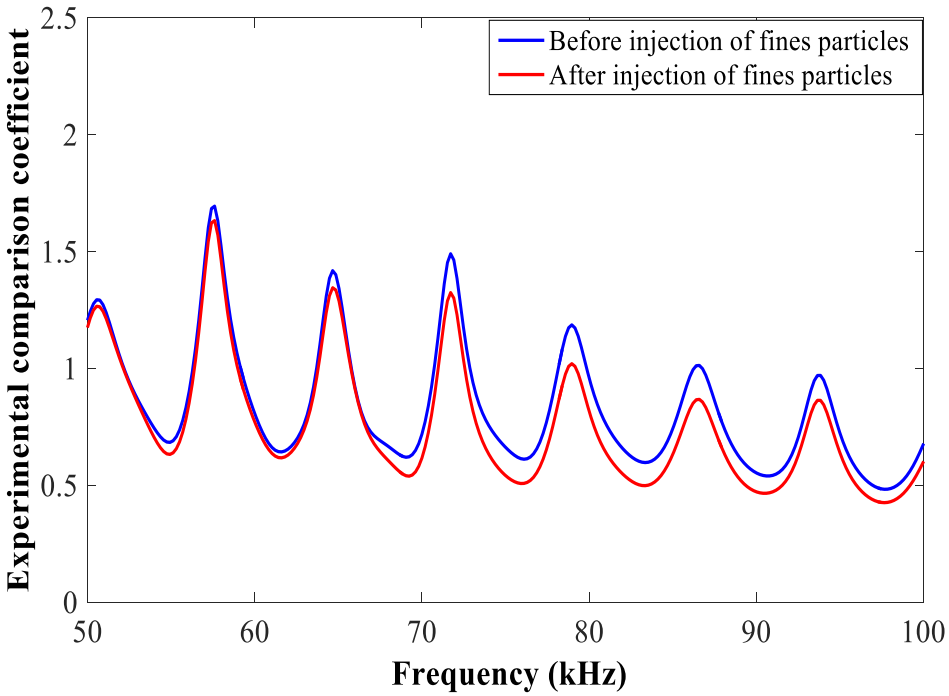

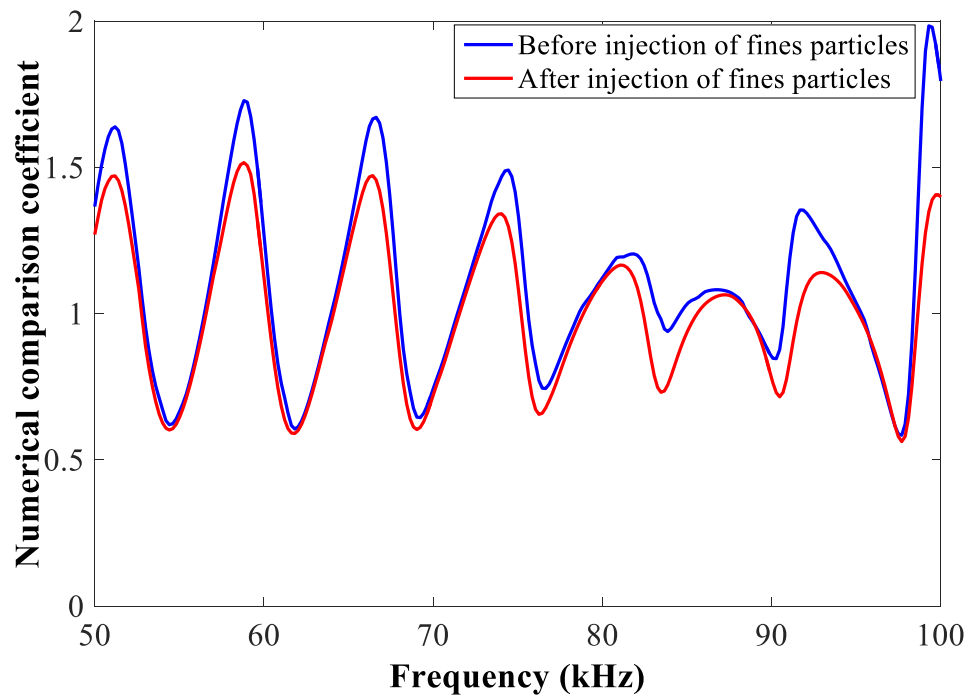

Sensitivity of the acoustic measures to the clogging phenomenon

Conclusions

- Particularities observed for the fundamental modes in the dispersion curves of a dpp layer compared to an elastic layer.

- The third dilatational wave plays no role for the characterisation of the Lamb waves in this frequency range.

- This analytical study can be also of interest as a first approach for understanding the acoustic behaviour of cancellous bones (media with multiple porosities).

- The study of clogging by ultrasonic methods can lead subsequently to the development of non destructive methods of predicting phenomena affecting hydraulic structures.

Thank you for your attention